Plant, Cell and Environment (2008) **31**, 378–391 doi: 10.1111/j.1365-3040.2007.01772.x

Short-term responses of leaf growth rate to water deficit scale up to whole-plant and crop levels: an integrated modelling approach in maize

KARINE CHENU[1], SCOTT C. CHAPMAN[2], GRAEME L. HAMMER[3], GREG MCLEAN[4], HALIM BEN HAJ SALAH[5] & FRANÇOIS TARDIEU[1]

[1]INRA, UMR 759 LEPSE, 2 place Viala, 34060 Montpellier Cedex 01, France, [2]CSIRO Plant Industry, St Lucia, Qld 4072, Australia, [3]APSRU, School of Land, Crop and Food Sciences, University of Queensland, Brisbane, Qld 4072, Australia, [4]APSRU, Department of Primary Industries and Fisheries, Toowoomba, Qld 4350, Australia and [5]INAT, Laboratoire d'agronomie, 43 Avenue CharlesNicolle 1002 Tunis, Tunisie

ABSTRACT

Physiological and genetic studies of leaf growth often focus on short-term responses, leaving a gap to whole-plant models that predict biomass accumulation, transpiration and yield at crop scale. To bridge this gap, we developed a model that combines an existing model of leaf 6 expansion in response to short-term environmental variations with a model coordinating the development of all leaves of a plant. The latter was based on: (1) rates of leaf initiation, appearance and end of elongation measured in field experiments; and (2) the hypothesis of an independence of the growth between leaves. The resulting whole-plant leaf model was integrated into the generic crop model APSIM which provided dynamic feedback of environmental conditions to the leaf model and allowed simulation of crop growth at canopy level. The model was tested in 12 field situations with contrasting temperature, evaporative demand and soil water status. In observed and simulated data, high evaporative demand reduced leaf area at the whole-plant level, and short water deficits affected only leaves developing during the stress, either visible or still hidden in the whorl. The model adequately simulated whole-plant profiles of leaf area with a single set of parameters that applied to the same hybrid in all experiments. It was also suitable to predict biomass accumulation and yield of a similar hybrid grown in different conditions. This model extends to field conditions existing knowledge of the environmental controls of leaf elongation, and can be used to simulate how their genetic controls flow through to yield.

Key-words: crop model; development; leaf area; leaf elongation; temperature; vapour pressure deficit; water deficit.

Abbreviations: LAI, leaf area index; LER, leaf elongation rate; PPFD, photosynthetic photon flux density; QTL, quantitative trait locus; VPD, vapour pressure deficit.

Correspondence: F. Tardieu. Fax: +33 (0)467 522 116; e-mail: tardieu@supagro.inra.fr

INTRODUCTION

Because leaf growth is one of the first processes affected by changes in temperature or plant water status (Boyer 1970; Ong 1983; Saab & Sharp 1989), many physiological studies have concentrated on short-term responses and associated mechanisms. They have demonstrated the roles of cellular processes such as controls of the cell cycle (Granier, Inzé & Tardieu 2000; Rymen *et al.* 2007), cell wall mechanical properties (Cosgrove 2005; Muller *et al.* 2007) or hydraulic properties of growing cells (Tang & Boyer 2002; Bouchabké, Tardieu & Simonneau 2006). However, the genetic controls of processes at this cellular level cannot be directly integrated into whole-plant models (Tardieu 2003). The interactions among these processes and their linkages to responses at whole-plant level are insufficiently understood, so that modelling each cellular response would result in a large number of redundant mechanisms and an overparameterization of the model.

A gap has thus developed between the current knowledge in plant physiology and the algorithms used in crop models. The latter are nevertheless needed to evaluate the effects of individual processes or genes on the seasonal dynamics of crop water use and carbon assimilation (Chapman *et al.* 2002; Yin, Struik & Kropff 2004). In crop models, the amount of new leaf area appearing each day is typically modelled either as a function of carbon availability to leaves (Goudriaan & van Laar 1994; Lizaso, Batchelor & Westgate 2003) or as a temperature-driven growth affected by limiting stress functions (Hammer, Carberry & Muchow 1993). These procedures are appropriate to simulate yield at large spatial scales or the effects of crop management (e.g. Lyon *et al.* 2003), but they are not sufficiently accurate to capture genetic variation in processes like leaf growth (Hammer *et al.* 2006). Some crop models now propose linkage between cultivar-specific parameters and associated genes or QTL, but these approaches have been applied either to constitutive traits (e.g. phenology; Chapman *et al.* 2003; Yin *et al.* 2005) or to binary traits related to environmental triggers (e.g. flowering response to photoperiod; Leon, Andrade & Lee 2000; Hoogenboom, White & Messina 2004).

An approach has been developed to fill this gap for maize leaf growth challenged by environmental conditions (Reymond *et al.* 2003; Sadok *et al.* 2007). It consisted, firstly, of expressing all rates per unit thermal time, thereby obtaining temperature-independent rates (Granier *et al.* 2002; Sadok *et al.* 2007). Secondly, the major environmental conditions involved in leaf development were identified for short time intervals (minutes to hours). Temperature, evaporative demand and soil water deficit had an overriding effect on leaf growth rate, whereas light and plant carbon balance had minor effects (Ben Haj Salah & Tardieu 1996, 1997; Sadok *et al.* 2007). Thirdly, response curves of LER to temperature, evaporative demand and soil water status were established, and the parameters of these responses were analysed genetically (Reymond *et al.* 2003; Welcker *et al.* 2007). This allowed simulation of leaf growth in novel inbred lines as defined by their alleles at QTLs (Reymond *et al.* 2003; Sadok *et al.* 2007). However, this method was applied only to one leaf position (leaf 6) and to simple environment scenarios, and therefore did not capture the integration to the whole-plant level nor complex interactions of plants with their environment (e.g. feedback of leaf growth on soil water depletion).

The aim of this study was to scale up this single-leaf model to the whole-plant and crop levels, and hence provide the capability to predict crop level consequences of the genetic variability in leaf growth response to environment. To achieve this, the single-leaf model was combined with a model that co-ordinates growth of all leaves of a plant, based on current knowledge of leaf development and on field experiments. This modified model took into account: (1) the parameters of response curves established in controlled conditions; and (2) a field-based developmental model presented here and parameterized in one field experiment. The resulting framework was implemented in the generic crop model of the APSIM platform to introduce dynamic feedback effects on leaf growth (via transpiration and soil water uptake). The model was then tested in 12 field environments with contrasting temperature, evaporative demand and water deficit conditions. Incorporating these approaches to leaf growth and development within the generic APSIM model also allowed prediction of biomass accumulation and crop yield in three field environments.

THEORY

Modelling the area of all individual leaves of a plant requires estimation of the beginning, the rate and the end of growth of each leaf, as well as the responses of these variables to environmental conditions. If only three environmental conditions and one parameter for each variable are considered (resulting in an oversimplification of the model), this would result in nine parameters per leaf position, i.e. 135 parameters for a 15-leaf plant. Hence, we seek a more parsimonious approach based on existing knowledge of leaf development.

Timing of leaf elongation

Leaves are initiated on the meristem at regular intervals of thermal time, i.e. time corrected for the temperature effect (Granier & Tardieu 1998; Lafarge & Tardieu 2002). Leaf elongation of monocotyledons is restricted to a zone near the leaf insertion point (Schnyder, Nelson & Coutts 1987; Ben Haj Salah & Tardieu 1995). As a consequence, leaf elongation is exponential (i.e. with a rate proportional to leaf length) until the elongating zone reaches its final length, and linear (i.e. rate independent of leaf length) afterwards, until final leaf length is achieved (for details, see Muller, Reymond & Tardieu 2001). The first two working hypotheses of our model were that (hypothesis 1) only the parameters characterizing the linear phase are needed because the exponential phase can be summarized by the date of transition and the length of the elongating zone, and (hypothesis 2) the dates of transition and end of expansion are linearly related to thermal time for the successive leaves of the plant.

In contrast to most existing studies, we considered the whole period of leaf development from leaf initiation to end of elongation, regardless of whether a leaf was visible or hidden in the whorl. Leaf tip and ligule appearances were therefore not considered *per se* in the simulation of leaf growth. They were only used in the final model to estimate the green leaf area for calculations of transpiration, light interception and biomass accumulation.

Leaf elongation rate

LER is constant per unit thermal time in the absence of environmental stresses (Sadok *et al.* 2007) because the distribution of the elongation rate in the growth zone is temperature independent (Tardieu *et al.* 2000). The maximum LER would be unique for all leaves of a plant if the distribution of growth within the elongating zone was common to all leaves, and would otherwise differ among leaves. Andrieu, Hillier & Birch (2006) showed that the maximal LER depends on the leaf rank, but as far as we know, the growth distribution within the elongation zone has never been compared among leaf positions. We used here an indirect method to simultaneously estimate the maximum LER and the lag time between leaf initiation and beginning of the linear elongation phase (duration of the exponential phase), which both depend on the length of the elongating zone.

Although the lamina and the sheath have different roles in the mature leaf, they have a common growth behaviour. In the developing leaf, the ligule crosses the elongating zone without change in the growth distribution (Muller *et al.* 2001). The transition from lamina to sheath expansion therefore occurs with a decrease in lamina elongation rate that is exactly compensated by the increase in sheath elongation rate, so that the elongation rate of the whole leaf is constant from the beginning of linear elongation until the end of the sheath elongation (Lafarge, de Raïssac & Tardieu 1998). Analyses of the environmental responses of LER

were therefore performed for the entire leaf (lamina and sheath) development period.

Previous studies have shown that changes in evaporative demand affect LER linearly even in the absence of water deficit (Acevedo *et al.* 1979; Ben Haj Salah & Tardieu 1996) and that a water deficit affects LER proportionally to predawn leaf water potential in the absence of evaporative demand. These effects can be combined in Eqn 1, originating from Reymond *et al.* (2003) with, in addition, the effect of the leaf rank:

$$\mathrm{LER}_k = \alpha_k(T - T_0)(a + b\mathrm{VPD}_{\mathrm{eq}} + c\Psi) \quad (1)$$

where LER_k is the LER of the leaf of rank k, T is the meristem temperature, $\mathrm{VPD}_{\mathrm{eq}}$ is the meristem to air VPD corrected for the effect of light on stomatal conductance, Ψ is the predawn leaf water potential and T_0 is the x-intercept of the relationship between LER and temperature. For a given leaf position, the parameters a, b and c are genotype dependent and unique across a range of experimental conditions. The term α_k accounts for the effect of the leaf rank (k).

The second set of working hypotheses for the model was that (hypothesis 3) the elongation rate on a given day is independent of that on the previous day (Sadok *et al.* 2007), (hypothesis 4) the different leaves of a plant behave independently from each other and (hypothesis 5) the sensitivities to evaporative demand and to soil water status (coefficients b and c) are common to all leaves of a plant.

MATERIALS AND METHODS

Plant material and growth conditions

Maize seeds (*Zea mays* L., single-cross hybrid Dea) were sown in the field in Grignon (northern France; 48°51′ N, 1°58′ W), Montpellier (southern France; 43°38′ N, 3°52′ W) and Mauguio (southern France; 43°36′ N, 3°58′ W) in deep, loamy soils between 1992 and 1998 under well-watered or water-deficient conditions (Table 1). In Montpellier and Mauguio, plants of well-watered treatments were watered so that their predawn leaf water potential never declined below –0.1 MPa. No irrigation was needed in Grignon. For water-deficit treatments, irrigation was stopped after sowing in Montpellier and Mauguio (MP94jl, MP95jn and MP95jl). In Grignon (GR92ap), a mobile shelter was placed over the plants during rainy periods to prevent water entry. In 1994, a crop was grown from 15 April to end of June to deplete soil water in such a way that the experiment sown in July (MP94jl) experienced an early water deficit.

Three field experiments were carried out in Gatton (Australia, 27°34′ S, 152°20′ E) on the hybrid Hycorn 53 (Pacific Seeds, Toowoomba, Australia) to test the model at crop level. Plants were sown on three dates and were grown under fully irrigated conditions (Table 1; Lemaire *et al.* 2007).

Maize plants were also grown in growth chamber and greenhouse experiments to analyse the responses of expansion rate of leaf 6 to temperature, VPD and predawn leaf water potential (non-destructively estimated from soil water content). These experiments (Ben Haj Salah & Tardieu 1995; Reymond 2001; Reymond *et al.* 2003) were used to estimate the parameters of responses (parameters a, b and c; Eqn 1) in the hybrid Dea.

Environmental measurements and variables

Air temperature and relative air humidity were measured with a thermohygrometer (HMP35A; Vaisala Oy, Helsinki, Finland) shaded from incident radiation and located in

Table 1. Characteristics of the field experiments

Exp	Location	Sowing date	Treatment	Density (pl m^{-2})	Irradiance (MJ m^{-2})	Rain (mm)	Temperature (°C)	$\mathrm{VPD}_{\mathrm{m\text{-}a}}$ (kPa)
GR92ap	Grignon, France	27 April 1992	Well watered	9	21.1	62	15.6	1.10
GR92ap	Grignon, France	27 April 1992	Water deficit	9	21.1	0	15.6	1.11
MP94jl	Montpellier, France	19 July 1994	Well watered	9	20.7	30	24.8	2.55
MP94jl	Montpellier, France	19 July 1994	Water deficit	9	20.7	30	24.8	2.66
MP95ma	Montpellier, France	16 May 1995	Well watered	12	22.7	39	20.0	1.49
MP95jn	Montpellier, France	20 June 1995	Well watered	12	23.9	13	24.0	1.95
MP95jn	Montpellier, France	20 June 1995	Water deficit	12	23.9	13	24.0	2.05
MP95jl	Montpellier, France	10 July 1995	Well watered	12	21.6	88	24.7	2.07
MP95jl	Montpellier, France	10 July 1995	Water deficit	12	21.6	88	24.7	2.09
MA97ma	Mauguio, France	14 May 1997	Well watered	8	19.1	151	19.5	1.36
MA97jn	Mauguio, France	18 June 1997	Well watered	8	21.3	65	22.0	1.60
MA98ma	Mauguio, France	20 May 1998	Well watered	8	23.0	47	21.1	1.70
GA99fv	Gatton, Australia	19 February 1999	Well watered	6.7	16.6	106	23.4	1.36
GA99sp	Gatton, Australia	16 September 1999	Well watered	6.7	10.4	156	20.1	1.28
GA01jv	Gatton, Australia	4 January 2001	Well watered	6.9	21.6	204	25.6	1.71

Irradiance (short wave solar), temperature (air temperature), $\mathrm{VPD}_{\mathrm{m\text{-}a}}$ (vapour pressure difference between meristem and atmosphere) were averaged for the period from sowing to flowering. Rain corresponded to cumulated rainfall from sowing to flowering.

the fields. Meristem temperature was measured using thermocouples (copper-constantan, 0.4 mm diameter) located inside the stem near the meristematic zone of non-measured plants. Incident light on plants was measured using a PPFD sensor (LI-190SB, Li-Cor, Inc, Lincoln, NE, USA). Measurements were logged every 20 s and averaged every 600 s (CR10X; Campbell Scientific, Inc, Shepshed, UK). A corrected VPD between meristem and air was calculated to take into account the effect of the PPFD on stomatal conductance. At PPFD less than 500 μmol m^{-2} s^{-1}, the corrected VPD was proportionally reduced to become 0 when PPFD was 0 (Reymond *et al.* 2003). Thermal time (°Cd) was calculated by integration of the difference between the mean meristem temperature and a threshold base temperature (T_0) of 10 °C (Ben Haj Salah & Tardieu 1995). The average environmental conditions corresponding to each field experiment are presented in Table 1.

In water deficit experiments, the soil water characteristics (upper and lower limits of plant extractable water) were determined from records of soil water content when the soil was fully wet, and after an extended period of extraction (Meinke, Hammer & Want 1993).

Plant measurements and variables

In the field experiments MA97ma, MA97jn and MA98ma (Table 1), 120 plants distributed in the field and more than 1 m apart were tagged at the three-leaf stage on one day. These plants displayed similar developmental stages over the whole period studied. On each plant, leaves 5 and 10 were marked soon after appearance to prevent any mistake in leaf counting because of senescence of the first leaves. Non-destructive measurements were recorded on 10 of these plants during the whole season. Their number of visible and ligulated leaves were recorded every third day. Their final lamina lengths and maximal widths were measured at the 10-leaf stage for leaves 1–6, and at silking for leaves 7–16. Destructive measurements were performed on five to eight of the remaining tagged plants every second or third day. These plants were dissected under a microscope (Leica wild F8Z stereomicroscope, Leica, Wetzlar, Germany) coupled to a video camera (Sony, CCD-IRIS/RGB, Tokyo, Japan) to count the number of leaves initiated (above 50 μm in length). Lamina lengths of all initiated leaves were determined with an image analyser (Bioscan-Optimas V4.10, Edmonds, WA, USA) for early developmental stages and with a ruler once leaf length exceeded 4 mm. The dates of beginning and end of the linear lamina elongation phase, and the mean lamina elongation rate over this period were determined for each leaf from a two-phase fit, thus distinguishing exponential and linear phases as described by Andrieu *et al.* (2006).

In the other experiments carried out in France (Table 1), 10 plants per treatment were tagged at the three-leaf stage, and their leaves 5 and 7 were marked few days after their appearance. Numbers of visible and ligulated leaves were recorded every third day, and their final leaf length and width were measured as described earlier. Predawn leaf water potential was measured every week in each treatment with a pressure chamber (Soil Moisture Equip. Corp., Santa Barbara, CA, USA).

In three experiments carried out in Australia, leaf, grain and whole-plant biomass were sampled on 10 plants every 3–4 weeks from a 1.44 to 1.50 m^2 quadrat. LAI was estimated from these plants as the product of total leaf weight (g m^{-2}) and specific leaf area (cm^2 g^{-1}). The latter was determined on a subsample of leaves from leaf area measured with an electronic planimeter.

Modelling

The model of leaf growth and development was based on the experimental data collected in this study. Leaf initiation; tip appearance; ligule appearance; and the beginning, rate and end of linear expansion were estimated for each leaf using data from the field experiments. The response of LER to temperature, VPD and soil water deficit were determined from experiments in the growth chamber and greenhouse. Detail of the leaf growth and development model is presented in Results.

The leaf model was incorporated as a replacement module for canopy leaf development in the APSIM-Maize model of the APSIM platform (Wang *et al.* 2002; Keating *et al.* 2003), version 5.2. The complete APSIM cropping system simulation platform is documented at www.apsim.info, and a detailed description and validation of the maize model is given at www.apsim.info/apsim/Publish/apsim/maize/docs/maize_science.htm. The incorporation of the leaf model allowed simulation of traits at canopy level and estimation of leaf environmental variables needed for the leaf model. A new micrometeorological module was added to APSIM to calculate weather data at an hourly time step. The temporal profile of temperature was estimated from Parton & Logan (1981). VPD was calculated from hourly air temperature and a dew point temperature estimated every day from minimum and maximum relative humidity and air temperature. Daily meristem temperature was input into the model for well-watered conditions. Drought impact on meristem temperature was estimated via a function depending on the hourly ratio of potential water uptake from the soil to water demand of the plant, which is an indicator of crop water status (Chapman, Hammer & Meinke 1993). The simulated hourly values of environmental variables closely resembled the actual data (e.g. VPD_{eq}, $y = 1.003$, $x - 0.017$, $r^2 = 0.838$). Predawn leaf water potential (ψ, MPa) was estimated from the fraction of transpirable soil water (FTSW) that was calculated from the soil water balance in APSIM [$\psi_l = \min(-0.1, -0.06 + 0.25 \ln(\text{FTSW})$].

The ability of the integrated model to simulate canopy leaf area development, biomass accumulation and grain yield was tested using data from experiments conducted in Australia (Table 1).

RESULTS

First experimental base of the model: stable patterns over a large range of environmental conditions provide a time frame for leaf development

The average calendar time necessary for two successive leaves to reach a stage of development varied between experiments. For instance, the time between the appearance of two successive leaves ranged from 2.8 to 7.4 d (Exp MP94jl and GR92ap), because of large differences in temperature among experiments (Table 1). However, all of the stages occurred on a regular basis in terms of thermal time, with timings common to all experiments (Fig. 1a). Successive leaves initiated every 21 ± 2 °Cd, and emerged from the whorl every 42 ± 1 °Cd regardless of the experiment. In the following, all rates are expressed per unit thermal time, as allowed by the linear relationships between temperature and LER (Fig. 2b) or leaf appearance rate (not shown).

Leaves began to elongate at a constant rate when they reached a specific length, presumably that of the elongating zone, which increased from 4 to 10 cm with leaf rank (Fig. 1c). The transition between the exponential and linear phases occurred in successive leaves every 26 ± 2 °Cd (confirming hypothesis 1 in Theory), i.e. a rate slightly slower than that for initiation. Hence, the lag time between leaf initiation and beginning of linear elongation increased with leaf rank, presumably because of an increase in the length of the elongating zone. The elongation rate during the linear phase increased with leaf rank for the first eight leaves, was maximal for leaves 9–12, which are the longest leaves, and decreased for the top leaves, which elongated as slowly as 50% of that of the longest leaves (Fig. 1b). The end of leaf expansion preceded leaf ligule appearance with a constant lag time, except for the first leaves in which this lag increased with leaf rank. Its progression along the stem was slower for the first eight leaves (0.020 leaf °Cd^{-1}) than for the following five leaves (0.033 leaf °Cd^{-1}). In all experiments, the last four leaves ceased elongating lmost simultaneously.

Overall, striking features were that the coordination between the development of all leaves was common to several experiments (Fig. 1a), and that leaf development processes occurred at different rates (slopes of Fig. 1a) resulting in longer development periods for intermediate leaves than for older (bottom) and younger (top) leaves.

Second experimental base of the model: responses of leaf growth to evaporative demand and soil water deficit at leaf and whole-plant levels

LER per unit thermal time decreased linearly with meristem-to-air VPD in well-watered plants during the day (Fig. 2c). It also decreased linearly with predawn leaf water potential in the absence of evaporative demand during the night (Fig. 2d). Linear equations therefore accounted for

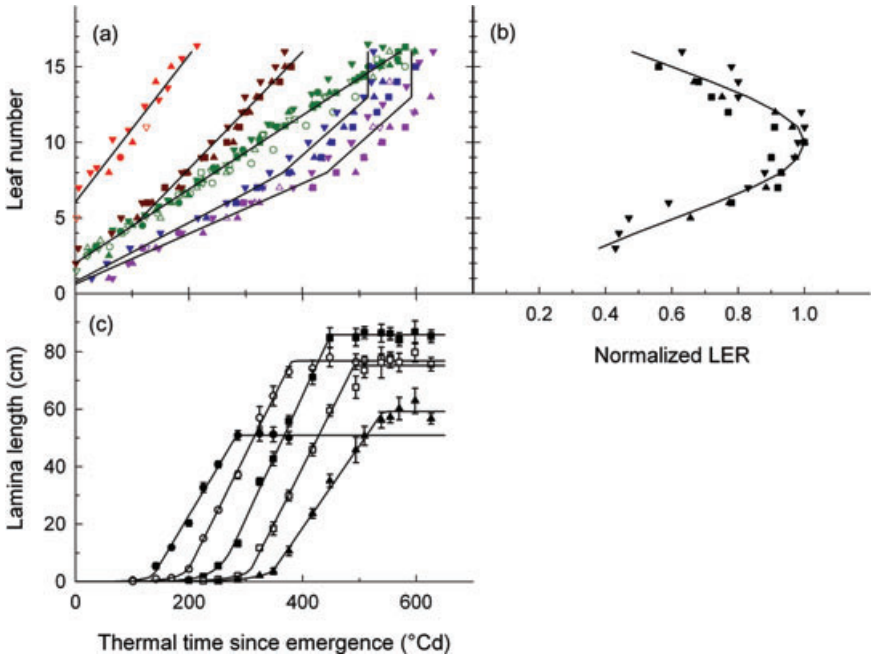

Figure 1. Leaf development in well-watered conditions. (a) Timings expressed in thermal time of leaf initiation (red), beginning of linear expansion (brown), leaf tip emergence (green), end of linear expansion (blue) and ligule appearance (purple) as a function of leaf rank. Experiments: GR92ap (open circle), MP94jl (open square), MP95ma (open triangle up), MP95jn (open triangle down), MP95jl (filled circle), MA97ma (filled square), MA97jn (filled triangle up), MA98ma (filled triangle down). (b) LER during the linear elongation phase, normalized by the maximum value for the profile, as a function of leaf rank. Same symbols as (a). (c) Change with thermal time in length of individual leaves from plant emergence, for leaves 6 (filled circle), 8 (open circle), 10 (filled square), 12 (open square) and 14 (filled triangle up) in Exp MA97jn. Points, observed data; lines, fitted relationships. Error bars, standard deviations; $n = 10$.

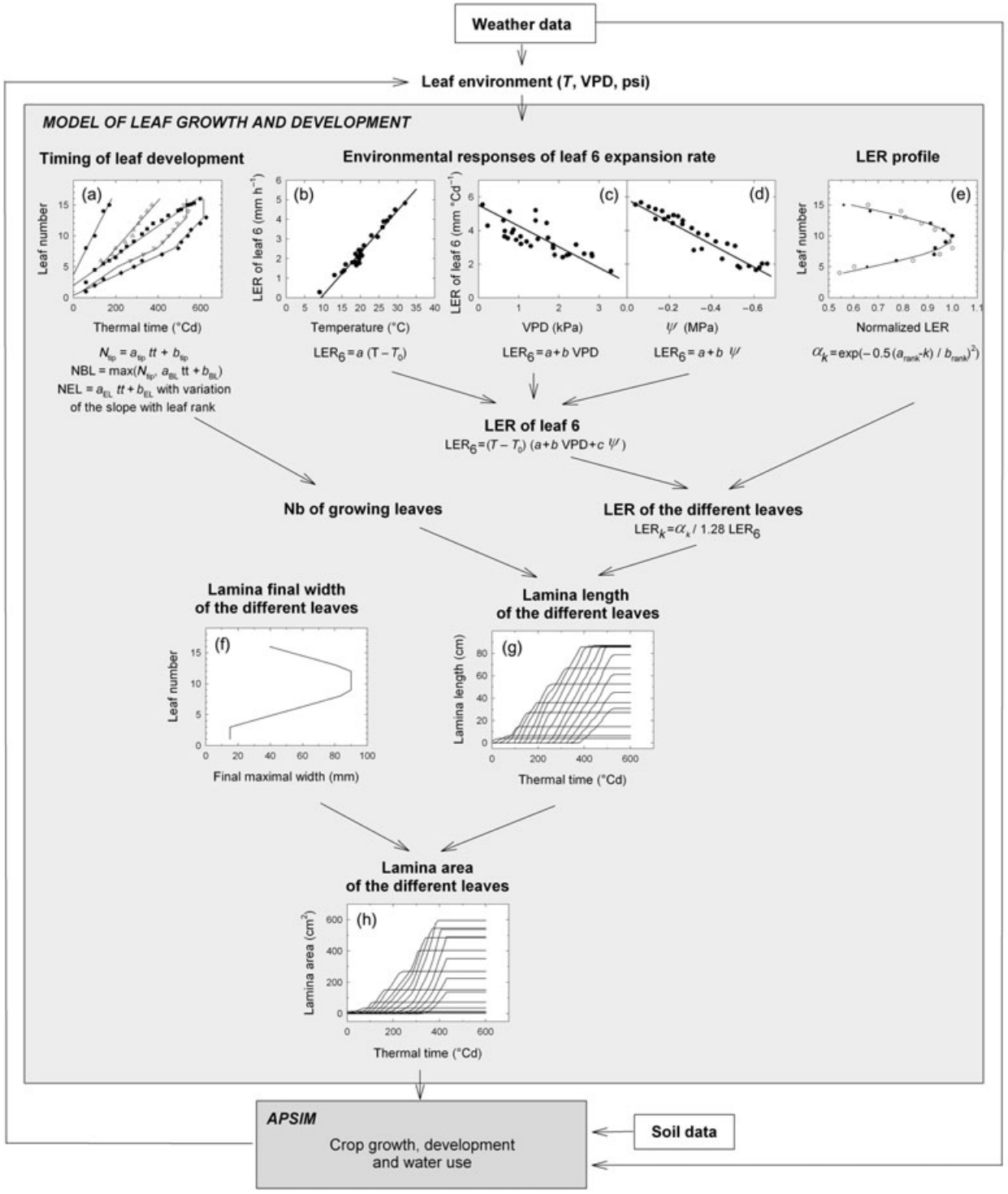

Figure 2. Schematic view of the interactions between the leaf model and the APSIM crop model. Data points presented in panels are those used for calibration of the model. (a) Change with thermal time in leaf initiation (filled circle), beginning of linear expansion (open triangle up), tip appearance (filled square), end of linear expansion (open triangle down) and ligule appearance (filled diamond) as a function of leaf rank. Data from Exp MA97jnWW. (b–e) Responses of LER of leaf 6 to meristem temperature (b), vapour pressure difference between meristem and air (VPD) (c), and predawn leaf water potential (ψ) (d). (e) LER during the linear expansion, normalized by the maximal value for the profile (values of α_k) as a function of leaf rank (k). Data from MA97jnWW (filled circle) and Andrieu *et al.* (2006) (open circle). (f) Final width of fully expanded lamina for all leaves of a plant. The model estimates the length (g) and area (h) of all leaves every hour. The green leaf area is input into the APSIM crop model which calculates from the climate and the crop development the soil water status and then the leaf environmental variables. The leaf environmental variables are used as input into the leaf growth model. Same abbreviations as in Table 2. (b, c, d).

the short-term response of leaf growth to VPD and predawn leaf water potential in the hybrid studied here (Eqns 8 & 9 in Table 2).

A large effect of evaporative demand on final leaf area was observed in field experiments, consistent with the effect on elongation rate in controlled conditions. Differences in evaporative demand accounted for the differences in leaf length among experiments for plants in well-watered treatments. In particular, an increase in mean meristem-to-air VPD of 1.1–2.6 kPa (averaged for the whole leaf development period) induced a large decrease in final leaf length (observed data points of Fig. 3).

Soil water deficit substantially reduced leaf length in four experiments (observed data points of Fig. 4). A detailed analysis of two experiments with different timings of water deficit is presented in Figs 5 and 6. In the first experiment (MP94jl), an early water deficit (characterized by the predawn leaf water potential) increased in intensity until 250 °Cd after emergence (Fig. 5a), while leaves 6–10 were developing with lamina either partly emerged or hidden in the whorl (Fig. 5b). Plants were then rewatered, so leaves 11–13 grew with no or moderate soil water deficit, and the last two leaves grew with an increasing water deficit. The differences in length between well-watered and stressed plants closely followed the timing of the water deficit (Fig. 5c). A large reduction in length was observed for young or old leaves that grew during the stress, whereas intermediate leaves 11–13, which grew under favourable

Table 2. Equations used in the leaf development model with their corresponding parameters and origin (either experiments presented here or references)

Process	Eqn	Equation	Parameter	Figure	Origin
Tip appearance	2	$N_{tip} = a_{tip} tt + b_{tip}$	$a_{tip} = 0.024$ °Cd^{-1} $b_{tip} = 2$	Fig. 2a	MA97jn
Beginning of linear expansion	3	$N_{BL} = \max(N_{tip}, a_{BL}\ tt + b_{BL})$	$a_{BL} = 0.039$ °Cd^{-1} $b_{BL} = 0.2$	Fig. 2a	MA97jn
End of linear expansion	4	$tt_{EL} = tt_{LL} - \text{lag}$ From leaves 1–5, $\text{lag} = (N_{EL} - 1)\alpha/(5 - 1)$ From leaf 5 to N_{final}, lag = l	$l = 80$ °Cd^{-1}	Fig. 2a	MA97jn
Ligule appearance	5	From leaf 1 to $(N_{final} - 8)$, $N_{LL} = a_{LL1} tt + b_{LL}$ From leaf $(N_{final} - 8)$ to $(N_{final} - 3)$, $N_{LL} = (N_{final} - 8) + a_{LL2}(tt - tt_{Nfinal-8})$ From leaf $(N_{final} - 3)$ to N_{final}, all appear at the same time $(tt_{LL} = tt_{Nfinal-3})$ with $tt_{Nfinal-8} = (N_{final} - 8 - b_{LL2})/a_{LL1}$	$b_{LL} = 0.3$ $a_{LL1} = 0.016$ °Cd^{-1} $a_{LL2} = 0.036$ °Cd^{-1} $N_{final} = 15$ or 16	Fig. 2a	MA97jn
Shape of LER profile	6	$\alpha_k = e^{-0.5\left(\frac{a_{rank}-k}{b_{rank}}\right)^2}$	$a_{rank} = 5.24$ $b_{rank} = 9.64$	Fig. 2e	MA97jn, Andrieu *et al.* (2006)
LER response to T	7	$\text{LER} = a(T - T_0)$	$a = 5.52$ mm °Cd^{-1} $T_0 = 10$ °C	Fig. 2b	Reymond (2001)
LER response to VPD	8	$\text{LER} = a + b$ VPD	$b = -1.25$ mm °Cd^{-1} kPa^{-1}	Fig. 2c	Reymond (2001)
LER response to ψ	9	$\text{LER} = a + c\ \psi_l$	$c = 6.5$ mm °Cd^{-1} Mpa^{-1}	Fig. 2d	Reymond (2001)
Leaf length at beginning of linear expansion		–	Mean value, 8 cm	–	MA97jn, Andrieu *et al.* (2006)
Final maximal leaf width	10	From leaves 1–3, $W = 15$ mm From leaf 4 to $(N_{max} - \text{plateau}/2)$, $W = 15 + a_{width}\ (N - 3)$ From leaf $(N_{max} - \text{plateau}/2)$ to $(N_{max} + \text{plateau}/2)$, $W = W_{max}$ From $(N_{max} + \text{plateau}/2)$ to N_{final}, $W = W_{max} - a_{width}\ (k - 3)$ where $N_{max} = 0.65\ N_{final}$ Plateau = $0.33\ N_{final} - 1.46$	$W_{max} = 90$ mm	Fig. 2f	Mean for all experiments

tt, thermal time since plant emergence; tt_{EL}, tt_{LL}, thermal time at the end of the linear expansion or at ligule appearance, respectively; N_{tip}, number of leaf tips appeared outside the whorl; N_{BL}, N_{EL} and N_{LL}, number of leaves which have begun linear elongation, stopped elongating or with appeared ligule, respectively; k, leaf rank; N_{final}, final leaf number; W, final maximum width of the considered leaf; W_{max}, final maximum width of the widest leaf of the plant; T, meristem temperature; VPD, meristem-to-air vapour pressure difference; ψ, predawn leaf water potential.

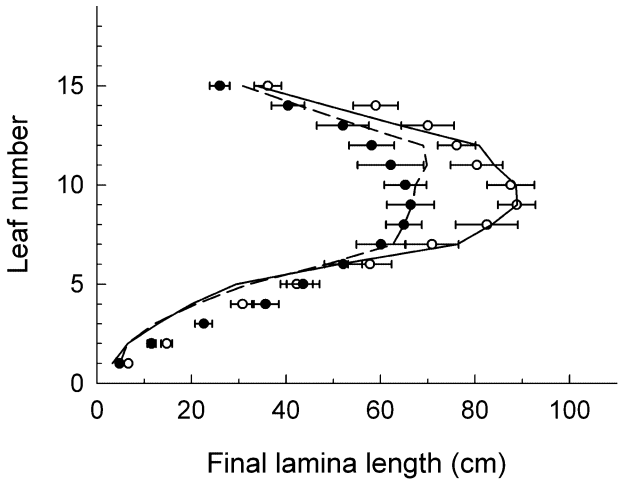

Figure 3. Observed and simulated final lamina lengths in plants grown with contrasting VPD. Data are for well-watered conditions in experiments GR92ap (open circle) and MP94jl (filled circle), with mean meristem-to-air VPD of 1.1 and 2.6 kPa, respectively, averaged during the vegetative period. Points, observed data; lines, simulated data. Error bars, standard deviations; $n = 10$.

conditions, showed small or no difference in length. In the second experiment (M95Jn), plants experienced a later but continuously increasing water deficit (Fig. 6). Consistently, no reduction in leaf length was observed for leaves 1–8, which grew under favourable conditions, whereas increasing effect of the deficit was observed for leaves 9–15. These observations indirectly confirm hypotheses inherent in the model (see Theory): (1) during the linear elongation phase, early developing leaves hidden in the whorl were as sensitive to water deficit as visible leaves; and (2) there was no 'after effect' of water deficit experienced by a given group of leaves on the later-appearing leaves, because leaves 11–13 were not affected by a stress that reduced the lengths of leaves 5–10 (Fig. 5).

Whole-plant model of leaf development and growth

The model presented in Fig. 2 resulted from the combination of equations that coordinate the development of all leaves of the plant (Fig. 2a,e; Eqns 2–6 in Table 2), with equations for response of the leaf 6 elongation rate to environmental conditions (Fig. 2b–d; Eqns 7–9 in Table 2). The changes in environmental conditions as sensed by leaves (meristem temperature, meristem-to-air VPD or predawn leaf water potential) were simulated using the APSIM model. Thirteen parameters were used for the model of leaf development at whole-plant level (Fig. 2a,e; Eqns 2–6 & 10). They were estimated from data of one experiment (MA97jn), combined with those of Andrieu *et al.* (2006) when possible. The four parameters of the environmental responses at the leaf level (Fig. 2b–d; Eqns 7–9) were estimated in greenhouse and growth chamber experiments,

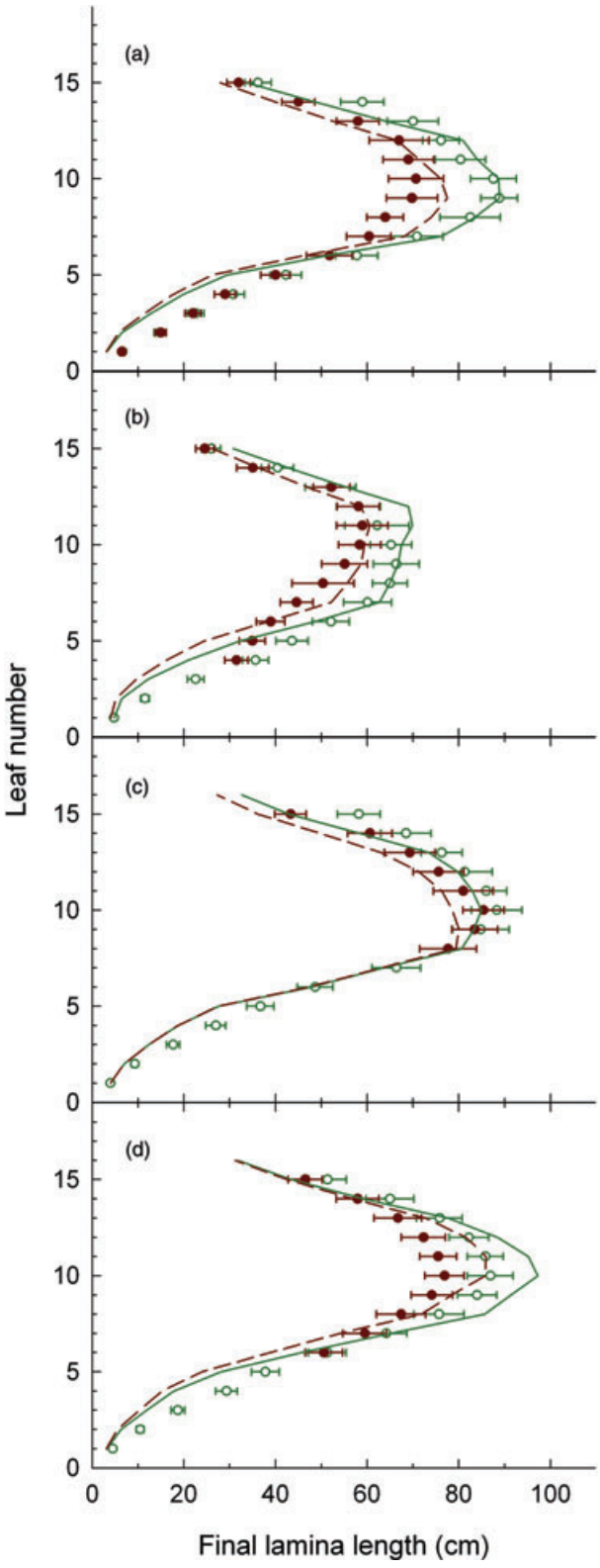

Figure 4. Observed and simulated final lamina lengths in plants grown with contrasting soil water status. Data from experiments GR92ap (a), MP94jl (b), MP95jn (c) and MP95jl (d). Points, observed data; lines, simulated data. (open circle, continuous line), well-watered conditions; (filled circle, dashes), water deficit conditions. Error bars, standard deviations 0.05; $n = 10$.

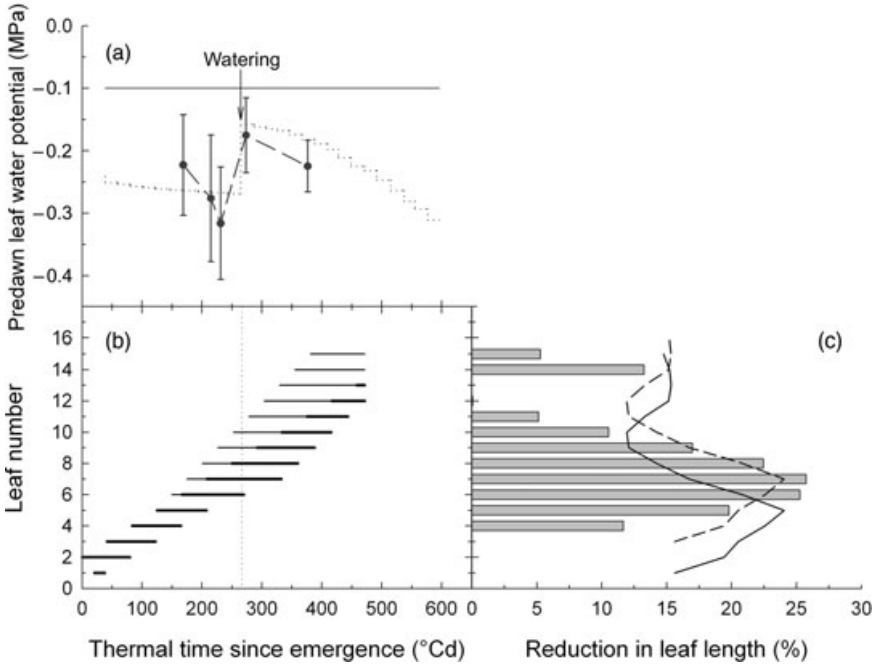

Figure 5. Observed and simulated effects of an early water deficit followed by watering on the final length of all leaves of a plant. (a) Change with thermal time in predawn leaf water potential in well-watered (continuous line) and water-deficit (filled circle, dots) treatments. Points, observed data; lines; simulated data. Observed data in the well-watered treatment are not shown for better legibility. Error bars, standard deviations. (b) Simulated timing of lamina elongation within (thin line) or outside (thick line) the whorl as a function of leaf rank. The vertical line indicates the time of watering. (c) Reduction in leaf length between well-watered and water-deficit treatments as a function of leaf rank. No observed data were available for the three first leaves. Bars, observed data; lines, simulated data. The dashed line in (c) corresponds to a simulation in which a stress-induced delay in leaf development was forced into the model. Data from MP94jl. The corresponding profile of final leaf length is presented in Fig. 4b. Error bars on predawn leaf water potential, standard deviations, $n = 8–10$.

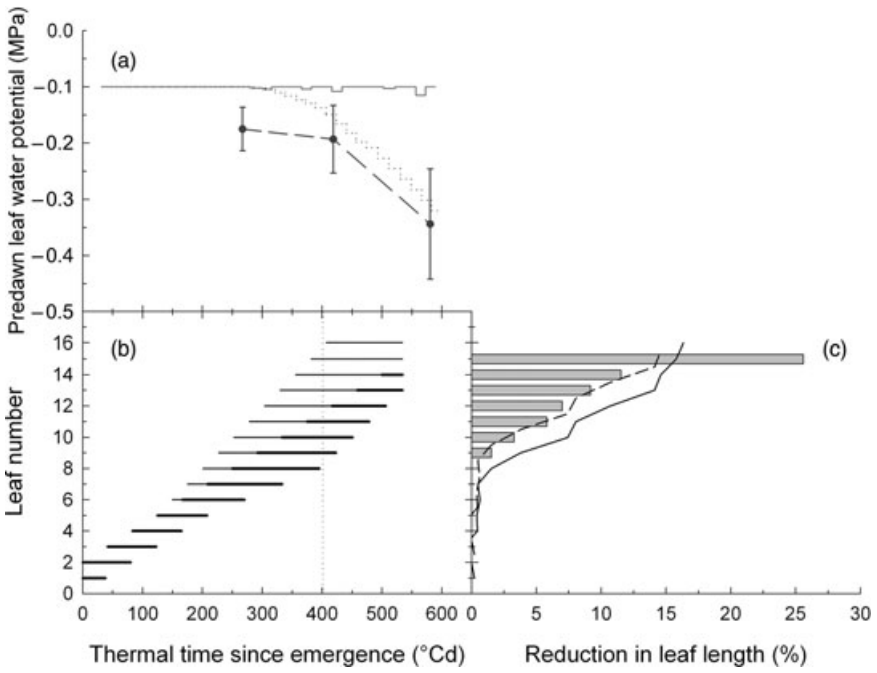

Figure 6. Observed and simulated effects of a late water deficit on the final length of all leaves of a plant. (a) Change with thermal time in predawn leaf water potential in well-watered (continuous line) and water-deficit (filled circle, dots) treatments. Points, observed data; lines; simulated data. Observed data in the well-watered treatment are not shown for better legibility. Error bars, standard deviations. (b) Simulated timing of lamina elongation within (thin line) or outside (thick line) the whorl, as a function of leaf rank. (c) Difference in leaf length between well-watered and water deficit treatments as a function of leaf rank. Bars, observed data; lines, simulated data. The dashed line in (c) corresponds to a simulation in which a stress-induced delay in leaf development was forced into the model. Data from MP95jn. The corresponding profile of final leaf length is presented in Fig. 4c. Error bars on predawn leaf water potential, standard deviations, $n = 8–10$.

independently of the field experiments. Other parameters of the APSIM model were unchanged compared with the current version 5.2 and can be found in www.apsim.info/apsim/Publish/apsim/maize/docs/maize_science.htm.

Leaf growth was calculated every hour for each leaf with the period of elongation restricted to the linear elongation phase, and with an initial length set at the estimated length of the elongating zone as proposed in Theory (hypothesis 1). The beginning of linear expansion and the end of elongation were determined via linear equations on thermal time (Fig. 2a; Eqns 3 & 4). The elongation rate of each leaf was calculated according to Eqn 1 (Fig. 2b–e), with the coefficient α_k (Eqn 1) which depended on leaf rank, and was determined via an exponential relationship (Fig. 2e; Eqn 6). Altogether, these equations allowed estimation of the change in leaf length with thermal time. Leaf width was estimated for each fully expanded leaf from the maximal leaf width value for the plant (maximal width of the largest fully expanded leaf, W_{max}) and from the number of leaves (Fig. 2f; Eqn 10). Leaf width growth was considered to occur during the linear elongation phase. Finally, lamina area (Fig. 2h) was calculated as the product of lamina length by maximal width, corrected by a shape factor of 0.75 (Zhang & Brandle 1997). The green leaf area (visible part of the leaf) was calculated every day as a fraction of the total leaf area by using the rates of leaf appearance and ligule appearance (Eqns 2 & 5). It was multiplied by plant density to calculate LAI, which was used by the APSIM model to simulate biomass accumulation and water use.

Simulation of leaf length profiles under contrasting environmental conditions

The model was used to simulate (with a single set of parameters) the final area of each leaf of a plant in the 12 experimental situations (Table 1). The experiments had a range in daily mean temperature of 15.6–24.7 °C, daily mean meristem-to-air VPD of 1.1–2.7 kPa and predawn leaf water potential of –0.05 to –0.4 MPa. Examples of simulations of final leaf length profiles are given for contrasting VPDs (Fig. 3) and water deficits (Fig. 4). Overall, the model adequately simulated the final lamina length (Fig. 7a) for the effects of both the environment and leaf position on the stem. The environmental effects are presented in Fig. 7a inset for the final length of a given leaf and in Fig. 7b for the total LAI. The model slightly underestimated the length of the first five leaves (Figs 3, 4 & 7), which collectively represented less than 6% of the final leaf area of the plant.

The simulations accurately reflected the experimental pattern of reduction in leaf length resulting from changes with time in soil water potential. In particular, only leaves exposed to water deficit during their development had a reduced final area in the model as in field experiments (Figs 5 & 6). However, compared with observed data, simulations of stress effects on leaf length were biased towards the bottom of the leaf profile. On inspection of the experimental data, there was a slower development rate in plants under water deficit compared with well-watered

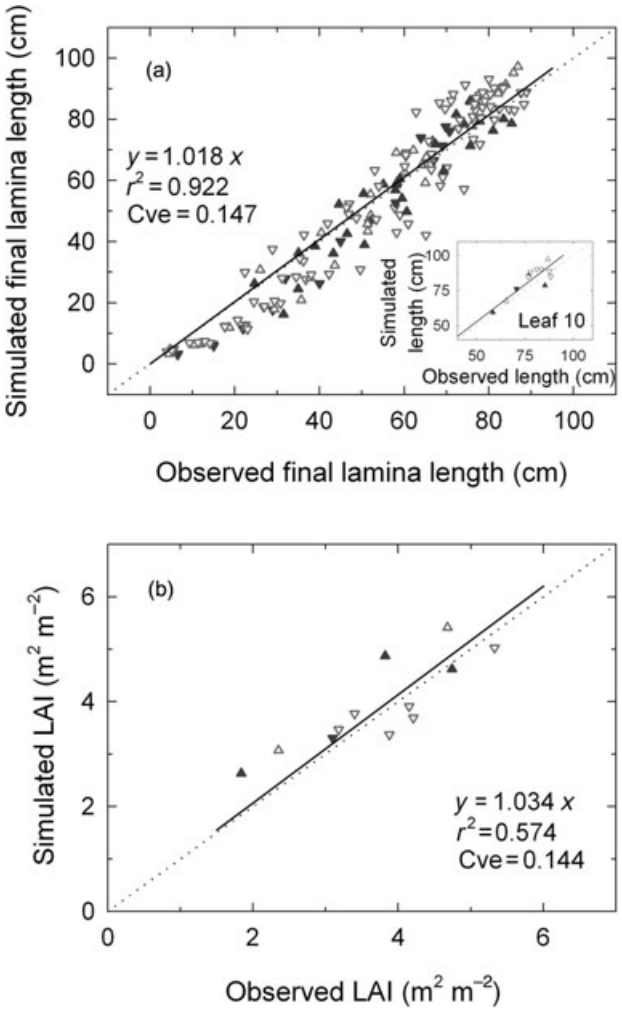

Figure 7. Comparisons of simulated versus observed data for final lamina length of all leaves (a), of leaf 10 only (a, inset) and of the total LAI (b) for well-watered (green open symbols) or water-deficit (red close symbols) conditions, with low meristem-to-air VPD (>2 kPa) (triangle down) or high meristem-to-air VPD (>2 kPa) (triangle up). Fits: (a), $y = 1.018\ x$, $r^2 = 0.922$, CVe = 0.147; (b), (a), $y = 1.034\ x$, $r^2 = 0.574$, CVe = 0.144. Dots, 1:1 line.

plants. This delay in development was not inserted in the model because of a current lack of biological basis, and to avoid the introduction of extra equations and parameters. Consequently, water deficits affected leaves at a later stage in the model than in the experiments. When the stress-induced delay in development was forced into the model, the observed and simulated differences in leaf length coincided.

The leaf growth model allowed calculation of crop biomass accumulation and yield via its interface with APSIM

The model was tested over the crop cycle in three experiments carried out in Australia with the hybrid Hycorn 53

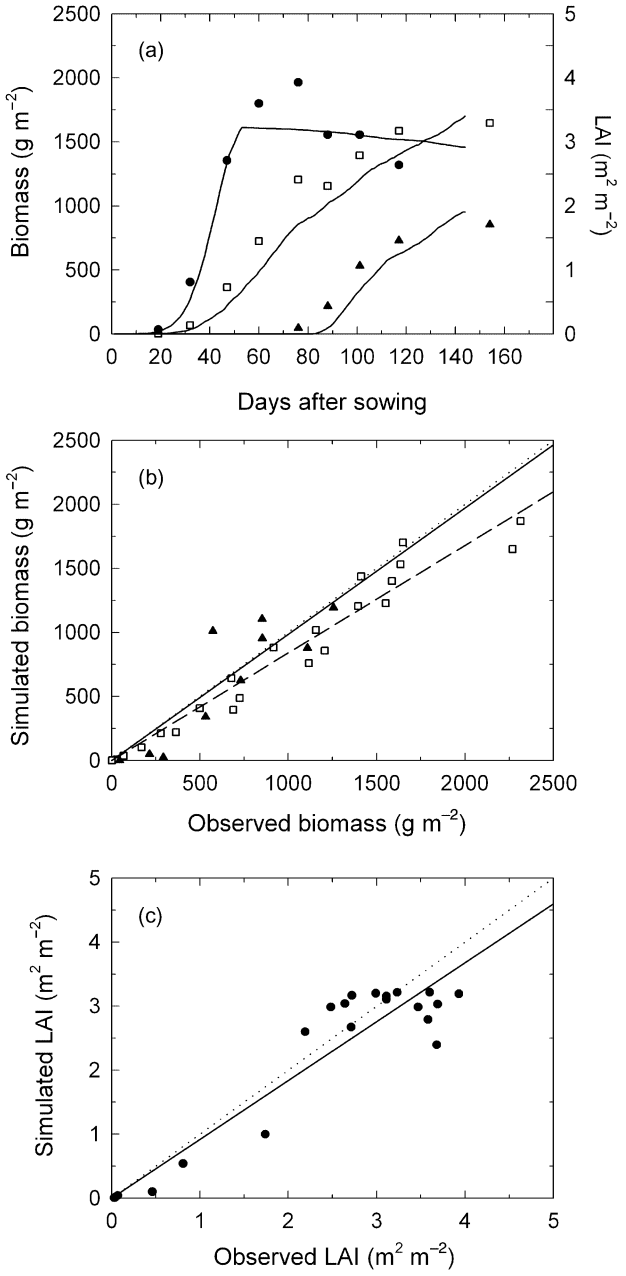

Figure 8. Simulation of plant development and growth of maize canopy in well-watered conditions. (a) Change with time in LAI, plant biomass and grain biomass. Points, observed data; lines, simulated data. (b,c) Comparison of simulated versus observed data for plant biomass and grain biomass (b) and LAI (c). Data from experiments GA99fv, GA99sp and GA01jv. (filled circle), LAI; (open square), plant biomass; (filled triangle up), grain biomass. Fits, (b), plant biomass (dashes), $y = 0.839\ x$, $r^2 = 0.955$, CVe = 0.177; grain biomass (continuous trait), $y = 0.986\ x$, $r^2 = 0.849$, CVe = 0.432; (c), LAI, $y = 0.919$, $r^2 = 0.619$, CVe = 0.347. Dots, 1:1 line.

(Fig. 8). This genotype had leaf growth similar to the hybrid Dea, but with longer lamina for the first leaves. The interface of the leaf model developed here with the crop model APSIM allowed estimation of integrated phenotypes at canopy level (Fig. 8a). The model adequately predicted LAI ($y = 0.919\ x$, $r^2 = 0.619$, CVe = 0.347), vegetative biomass ($y = 0.839\ x$, $r^2 = 0.955$, CVe = 0.177) and grain yield ($y = 0.986\ x$, $r^2 = 0.849$, CVe = 0.432) under well-watered conditions that varied in seasonal temperature and VPD profiles across contrasting sowing dates.

DISCUSSION

The model integrated short-term mechanisms into a crop modelling framework

Connecting models with different levels of integration (temporal and spatial scales) is the object of a long-lasting debate in the plant scientific community (Passioura 1996, 2007). Responses to environmental conditions often differ if they are considered over some hours, days or weeks, so it has been argued that each time scale is associated with its own set of overriding mechanisms, e.g. hydraulic processes over minutes to hours, carbon status over days, developmental processes over weeks (e.g. Munns *et al.* 2000). If this were true, it would be difficult to build an effective model that crosses time scales, so models designed to evaluate the consistency of known short-term mechanisms should be distinguished from those designed to make predictions and help in decision making at crop level (Passioura 1996). However, the study presented here shows that it is possible to integrate a leaf growth model with a time scale of hours into a canopy model with a time scale of months. This was possible because the models at short and longer time scales were specifically designed for this integration.

The model of leaf growth accounts for short-term changes in elongation rate as a response to environmental conditions, but does not attempt to directly include mechanisms such as changes in cell division, cell wall properties or hydraulic processes which cannot yet be scaled up (Tardieu 2003). The connection to physiological and molecular mechanisms is thus done *a posteriori*, via genetic analyses of individual responses to environmental conditions (Reymond *et al.* 2003; Welcker *et al.* 2007), or analyses of the contributions of traits such as turgor maintenance (Bouchabké *et al.* 2006), abscisic acid (Voisin *et al.* 2006) or expansins (Muller *et al.* 2007) to the changes in leaf growth.

The leaf developmental model predicts the beginning and end of linear elongation for each leaf and the variation in LER among leaves of the plant (parameter α_k; eqns 1 & 6). It therefore fixes the time frame of expansion, while the leaf growth model simulates the LER as affected by environmental conditions. Interfacing models would not have been possible if we had used a standard developmental model that only predicted the increase in green leaf area based on leaf tip and ligule appearances (e.g. Zur, Reid & Hesketh 1989; Keating *et al.* 2003).

The crop model APSIM, which has a thermal-time-driven programme of plant development, is compatible in its principles with the new leaf model. It was enhanced by introducing several novel features, namely (1) algorithms to derive hourly values of the environmental conditions based

on daily values; and (2) procedures to calculate micrometeorological variables and predawn leaf water potential from standard meteorological data interfaced with the model predictions of water use and crop water status. The crop model could therefore simulate the predawn leaf water potential (via soil water status), leaf temperature and evaporative demand at the time step required for the leaf growth model.

Stable patterns of leaf development allowed estimation of plant leaf area at whole-plant and canopy levels in contrasting environments

Models of development such as that presented in Fig. 2 have been applied in different species and for both reproductive and vegetative development (Zur *et al.* 1989; Ney & Turc 1993). A novelty of the model presented here lies in the developmental stages taken into account. A constant thermal time elapsed between the transition of the exponential to linear elongation phase for successive leaves. This validates hypothesis 2 of Theory. It is noteworthy that the estimated leaf length at which the transition occurred is compatible with published lengths of the elongating zone (Muller *et al.* 2001; Rymen *et al.* 2007). The pattern for cessation of elongation was more complex, probably because of the increasing influence of reproductive organs over plant development. The thermal time between the cessation of elongation in successive leaves decreased for leaves growing after floral transition. It was nullified for the top leaves, which developed during rapid growth of reproductive organs, consistent with data of Lafarge & Tardieu (2002) and Andrieu *et al.* (2006).

Several other novelties of the model are worth mentioning. (1) The responses to environmental conditions are unique for a given genotype in a wide range of experimental situations including field, greenhouse or growth chamber (Ben Haj Salah and Tardieu 1995; Reymond *et al.* (2003). Contrary to statistical stress functions usually used in crop models, these responses can therefore be considered as physiological traits with biological bases and be related to stable QTLs. (2) This is the first time to our knowledge that the direct effect of evaporative demand has been reported and used to simulate final leaf area. (3) Consistent with experimental results, leaves are considered as sensitive to their environment during the whole period of linear elongation, while they are either hidden in the whorl or emerged above it. This suggests a minor role of the exponential elongation phase in leaf developmental responses to water deficit compared to the linear phase, consistent with hypothesis 1 of the Theory. (4) The expansions of different leaves of the plant are considered as independent (hypothesis 3). This was consistent with the experiment presented in Fig. 6, where the reduction in growth of the first 10 leaves because of water deficit had no influence on the growth of the following leaves which grew under well-watered conditions. There was, therefore, no cumulative effect of the water deficit (hypothesis 4), which would have been expected if the reduction in leaf growth by the water deficit was because of a reduced carbon availability, as in the model of Lizaso *et al.* (2003).

Finally, we acknowledge that leaf width was less accurately modeled than leaf length, although its environmental variation is lower than that of leaf length (Reymond, Muller & Tardieu 2004).

Towards a model to estimate how genetic variability affects yield in a range of climatic conditions

Most of the parameters used in the leaf model are stable characteristics of the considered genotype, encapsulate the environmental effects and can be related to QTL independent of environment (Reymond *et al.* 2003; Welcker *et al.* 2007). This enables avoidance of complex QTL × environment interactions that are commonly observed for more complex traits such as leaf area or biomass accumulation (Yin *et al.* 1999; Reymond *et al.* 2004). Presently, the list of 'stable' traits related to leaf growth and development in maize includes the duration of the vegetative phase (Yin *et al.* 1999); leaf width (Reymond *et al.* 2004); and the maximum elongation rate and its responses to temperature, soil water status and evaporative demand (Reymond *et al.* 2003; Welcker *et al.* 2007). Other characters of the model, such as the duration of elongation, may be dissected genetically in the future. This study opens the way for modelling genetic variability at the whole-plant scale under fluctuating conditions. Hence, it should help in the evaluation of the contribution to yield of QTL for individual leaf traits, and thus contribute to breeding for these types of environments.

ACKNOWLEDGMENTS

We are grateful to C. Paysant, C. Thonat and A. Massignan for data from field experiments in France and in Australia. This project was funded by the Generation Challenge Programme, and by Arvalis, Institut du Végétal.

REFERENCES

Acevedo E., Fereres E., Hsiao T.C. & Henderson D.W. (1979) Diurnal growth trends, water potential and osmotic adjustment of maize and sorghum leaves in the field. *Plant Physiology* **64,** 476–480.

Andrieu B., Hillier J. & Birch C. (2006) Onset of sheath extension and duration of lamina extension are major determinants of the response of maize lamina length to plant density. *Annals of Botany* **98,** 1005–1016.

Ben Haj Salah H. & Tardieu F. (1995) Temperature affects expansion rate of maize leaves without change in spatial distribution of cell length. Analysis of the coordination between cell division and cell expansion. *Plant Physiology* **109,** 861–870.

Ben Haj Salah H. & Tardieu F. (1996) Quantitative analysis of the combined effects of temperature, evaporative demand and light on leaf elongation rate in well-watered field and laboratory-grown maize plants. *Journal of Experimental Botany* **47,** 1689–1698.

Ben Haj Salah H. & Tardieu F. (1997) Control of leaf expansion rate of droughted maize plants under fluctuating evaporative demand. A superposition of hydraulic and chemical messages? *Plant Physiology* **114,** 893–900.

Bouchabké O., Tardieu F. & Simonneau T. (2006) Leaf growth and turgor in growing cells of maize (*Zea mays* L.) respond to evaporative demand in well-watered but not in water saturated soil. *Plant, Cell & Environment* **29,** 1138–1148.

Boyer J.S. (1970) Leaf enlargement and metabolic rates in corn, bean and sunflower at various leaf water potential. *Plant Physiology* **46,** 233–235.

Chapman S.C., Hammer G.L. & Meinke H. (1993) A sunflower simulation model: I. Model development. *Agronomy Journal* **85,** 725–735.

Chapman S.C., Hammer G.L., Podlich D.W. & Cooper M. (2002) Linking biophysical and genetic models to integrate physiology, molecular biology and plant breeding. In *Quantitative genetics, Genomics, and Plant Breeding* (ed. M.S. Kang), pp. 167–187. CABI, Wallingford, UK/New York, NY.

Chapman S.C., Cooper M., Podlich D.W. & Hammer G.L. (2003) Evaluating plant breeding strategies by simulating gene action and dryland environment effects. *Agronomy Journal* **95,** 99–113.

Cosgrove D.J. (2005) Growth of the cell wall. *Nature Reviews. Molecular Cell Biology* **6,** 850–861.

Goudriaan J. & van Laar H.H. (1994) *Modelling Potential Crop Growth Processes*. Kluwer Academic Publishers, Dordrecht, the Netherlands.

Granier C. & Tardieu F. (1998) Is thermal time adequate for expressing the effects of temperature on sunflower leaf development. *Plant, Cell & Environment* **21,** 695–703.

Granier C., Inzé D. & Tardieu F. (2000) Spatial distribution of cell division rate can be deduced from that of p34 cdc2 kinase activity in maize leaves grown at contrasting temperatures and soil water conditions. *Plant Physiology* **124,** 1393–1412.

Granier C., Massonnet C., Turc O., Muller B., Chenu K. & Tardieu F. (2002) Individual leaf development in *Arabidopsis thaliana*: a stable thermal-time-based programme. *Annals of Botany* **89,** 595–604.

Hammer G.L., Carberry P.S. & Muchow R.C. (1993) Modelling genotypic and environmental control of leaf area dynamics in grain sorghum. I. Whole plant level. *Field Crops Research* **33,** 293–310.

Hammer G., Cooper M., Tardieu F., Welch S., Walsh B., Eeuwijk F., Chapman S. & Podlich D. (2006) Models for navigating biological complexity in breeding improved crop plants. *Trends in Plant Sciences* **11,** 587–593.

Hoogenboom G., White J.W. & Messina C.D. (2004) From genome to crop: integration through simulation modeling. *Field Crops Research* **90,** 145–163.

Keating B.A., Carberry P.S., Hammer G.L., *et al*. (2003) An overview of APSIM, a model designed for farming systems simulation. *European Journal of Agronomy* **18,** 267–288.

Lafarge T. & Tardieu F. (2002) A model coordinating the elongation of all leaves of a sorghum cultivar, applies to Mediterranean and Sahelian conditions. *Journal of Experimental Botany* **53,** 715–725.

Lafarge T., de Raïssac M. & Tardieu F. (1998) Elongation rate of sorghum leaves has a common response to meristem temperature in diverse African and European conditions. *Field Crop Research* **58,** 69–79.

Lemaire G., van Oosterom E., Sheehy J., Jeuffroy M.H., Massignam A. & Rossato L. (2007) Is crop N demand more closely related to dry matter accumulation or leaf area expansion during vegetative growth? *Field Crops Research* **100,** 91–106.

Leon A.J., Andrade F.H. & Lee M. (2000) Genetic mapping of factors affecting quantitative variation for flowering in sunflower. *Crop Science* **40,** 404–407.

Lizaso J.I., Batchelor W.D. & Westgate M.E. (2003) A leaf area model to simulate cultivar-specific expansion and senescence of maize leaves. *Field Crops Research* **80,** 1–17.

Lyon D.J., Hammer G.L., McLean G.B. & Blumenthal J.M. (2003) Simulation supplements field studies to determine no-till dryland corn population recommendations for semiarid western. *Nebraska Agronomy Journal* **95,** 884–891.

Meinke H., Hammer G.L. & Want P. (1993) Potential soil water extraction by sunflower on a range of soils. *Field Crops Research* **32,** 59–81.

Muller B., Reymond M. & Tardieu F. (2001) The elongation rate at the base of a maize leaf shows an invariant pattern during both the steady-state elongation and the establishment of the elongation zone. *Journal of Experimental Botany* **52,** 1259–1268.

Muller B., Bourdais G., Reidy B., Bencivenni C., Massonneau A., Condamine P., Rolland G., Conéjéro G., Rogowsky P. & Tardieu F. (2007) Association of specific expansins with growth in maize leaves is maintained under environmental, genetic, and developmental sources of variation. *Plant Physiology* **143,** 278–290.

Munns R., Passioura J.B., Guo J., Chazen O. & Cramer G.R. (2000) Water relation and leaf expansion: importance of the time scale. *Journal of Experimental Botany* **51,** 1495–1504.

Ney B. & Turc O. (1993) Heat-unit-based description of the reproductive development of pea. *Crop Science* **33,** 510–514.

Ong C.K. (1983) Response to temperature in a stand of pearl millet (*Pennisetum typhoides* S. & H.). IV. Extension of individual leaves. *Journal of Experimental Botany* **34,** 1731–1739.

Parton W.J. & Logan A. (1981) A model for diurnal variation in soil and air temperature. *Agricultural Meteorology* **23,** 205–216.

Passioura J.B. (1996) Simulation models: science, snake oil, education, or engineering? *Agronomy Journal* **88,** 690–694.

Passioura J.B. (2007) The drought environment: physical, biological and agricultural perspectives. *Journal of Experimental Botany* **58,** 113–117.

Reymond M. (2001) *Variabilité génétique des réponses de la croissance foliaire du maïs à la température et au déficit hydrique. Combinaison d'un modèle écophysiologique et d'une analyse QTL*. PhD thesis, Ecole Nationale Supérieure d'Agronomie de Montpellier, Montpellier, France.

Reymond M., Muller B., Leonardi A., Charcosset A. & Tardieu F. (2003) Combining quantitative trait loci analysis and an ecophysiological model to analyze the genetic variability of the responses of maize leaf growth to temperature and water deficit. *Plant Physiology* **131,** 664–675.

Reymond M., Muller B. & Tardieu F. (2004) Dealing with the genotype × environment interaction via a modelling approach: a comparison of QTLs of maize leaf length or width with QTLs of model parameters. *Journal of Experimental Botany* **55,** 2461–2472.

Rymen B., Fiorani F., Kartal F., Vandepoele K., Inze D. & Beemster G.T.S. (2007) Cold nights impair leaf growth and cell cycle progression in maize through transcriptional changes of cell cycle genes. *Plant Physiology* **143,** 1429–1438.

Saab I.N. & Sharp R.E. (1989) Non-hydraulic signals from maize roots in drying soil: inhibition of leaf elongation but not stomatal conductance. *Planta* **179,** 466–474.

Sadok W., Naudin P., Boussuge B., Muller B., Welcker C. & Tardieu F. (2007) Leaf growth rate per unit thermal time follows QTL-dependent daily patterns in hundreds of maize lines under naturally fluctuating conditions. *Plant, Cell & Environment* **30,** 135–146.

Schnyder H., Nelson C.J. & Coutts J.H. (1987) Assessment of

spatial distribution of growth in the elongation zone of grass leaf blades. *Plant Physiology* **85,** 290–293.

Tang A.C. & Boyer J.S. (2002) Growth-induced water potentials and the growth of maize leaves. *Journal of Experimental Botany* **53,** 489–503.

Tardieu F. (2003) Virtual plants: modelling as a tool for the genomics of tolerance to water deficit. *Trends in Plant Science* **8,** 9–14.

Tardieu F., Reymond M., Hamard P., Granier C. & Muller B. (2000) Spatial distributions of expansion rate, cell division rate and cell size in maize leaves. A synthesis of the effects of soil water status, evaporative demand and temperature. *Journal of Experimental Botany* **51,** 1505–1514.

Voisin A.S., Reidy B., Parent B., Rolland G., Redondo E., Gerentes D., Tardieu F. & Muller B. (2006) Are ABA, ethylene or their interaction involved in leaf growth response to soil water deficit? An analysis using naturally occurring variation or genetic transformation of ABA production in maize. *Plant, Cell & Environment* **29,** 1829–1840.

Wang E., Robertson M., Hammer G.L., Carberry P., Holzworth D., Meinke H., Chapman S.C., Hargreaves J., Huth N. & Campbell G.S. (2002) Development of a generic crop model template in the cropping system model APSIM. *European Journal of Agronomy* **18,** 121–140.

Welcker C., Boussuge B., Benciveni C., Ribaut J.M. & Tardieu F. (2007) Are source and sinks strengths genetically linked in maize plants subjected to water deficit? A QTL study of the responses of leaf growth and anthesis – silking interval to water deficit. *Journal of Experimental Botany* **58,** 339–349.

Yin X., Stam P., Johan Dourleijn C. & Kropff M.J. (1999) AFLP mapping of quantitative trait loci for yield-determining physiological characters in spring barley. *Theoretical and Applied Genetics* **99,** 244–253.

Yin X., Struik P.C. & Kropff M.J. (2004) Role of crop physiology in predicting gene-to-phenotype relationships. *Trends in Plant Science* **9,** 426–432.

Yin X., Struik P.C., Euwijk F., Stam P. & Tang J.J. (2005) QTL analysis and QTL-based prediction of flowering phenology in recombinant inbred lines of barley. *Journal of Experimental Botany* **56,** 967–976.

Zhang H. & Brandle J.R. (1997) Leaf area development of corn as affected by windbreak shelter. *Crop Science* **37,** 1253–1257.

Zur B., Reid J.F. & Hesketh J.D. (1989) The dynamics of a maize canopy development. I. Leaf ontogeny. *Biotronics* **18,** 55–66.

Received 10 July 2007; received in revised form 23 November 2007; accepted for publication 5 December 2007

